

Performance Investigation of a Photovoltaic Module Integrated with Different Optical Filters

A. Mostafa^{1,2}, S. E. Madbouly^{3,*}, M. Abd El-Hamid¹, E. Elgendy³

¹ Mechanical Power Engineering Department, Faculty of Engineering at El-Mattaria, Helwan University, Cairo, Egypt.

² Energy and Renewable Energy Engineering Program, Faculty of Engineering and Technology, Egyptian Chinese University.

³ Mechanical Engineering Department, College of Engineering and Technology-Cairo Campus, Arab Academy for Science, Technology and Maritime Transport (AASTMT), Egypt, elgenady@Egypt.aast.edu.

ABSTRACT

Currently, 10 to 25% of the solar energy that reaches the PV unit surface is transformed into electricity, with the rest being dissipated as heat. The efficiency of converting the incident solar radiation into electrical power is greatly influenced by the heat accumulation on the photovoltaic modules. Coupling the PV module with optical filters are considered to be one of the most promising techniques to dramatically raise the electrical efficiency. In the present investigation, two optical filters employing different static working fluids coupled with a PV module are designed and compared with the stand-alone PV module experimentally. The results find that the efficiency of the optical filter using water reaches to about 60.02%, which is higher than the optical filter employing glycerin by implementing the Monte Carlo approach. When the optical filters are combined with the PV unit, the electrical power output is increased by around 60 and 64%, respectively, when compared to the PV module without the optical filter.

Keywords: Photovoltaic module; optical filter; water optical fluid; glycerin optical fluid; Monte Carlo method.

*Corresponding Author madboulysalaheldin@gmail.com

1. INTRODUCTION:

Renewable energy resources have been found to be an optimal solution to eliminate the adverse impacts of fossil fuels on the environment along with facing the significant elevation in the gap between the energy demand and production resulting from the considerable increase of the world population. These resources include solar radiation, wind, geothermal, wave, and biofuel energies. Renewable energy usage has been dramatically elevated since 1950. The Photovoltaic module installed capacity has been expanded from approximately 14.8 to 150.83 TWh throughout the last 10 years, with an equal share to that of the wind energy, where both represent the highest share percentage among the renewable energy installations globally [1]. Thus, the recent increased installation of photovoltaic modules as a renewable and environmentally safe energy source with low maintenance costs is a motivating factor to devote significant attention for further efficiency improvement [2]. Unfortunately, only around 10 to 25% of the solar energy that strikes the PV unit surface is converted into electricity, with the excess being wasted as heat [3-5]. Whereas, this excess heat leads to a substantial PV surface temperature increase which is a main factor for the PV module power output reduction [6, 7]. The generated power and electrical conversion efficiency of the PV unit are declined by around 0.65 % and 0.4 to 0.65 %, respectively, for each one degree rise in temperature [8, 9]. Moreover, the portion of solar radiation which can be converted in to electricity lies in the wave length range of 400 ~ 1100 nm, however the wave lengths that range from 1100 to 2500 nm are converted to waste

heat [10, 11]. Spectrum beam splitting technology is one of the most promising approaches for overcoming the PV module performance constraints [12]. Whereas, absorptive-based filters are considered to be a reliable method that utilized an optical filter represented in a fluid located between the sun light and the PV module surface [13]. These filters are operated such that the spectrum is divided by enabling only certain wavelengths to flow through them, then directly transmitted to the PV cell, while the rest is absorbed directly by the filter as heat, and this is the portion that cannot be converted to electricity by the solar cell [14]. Furthermore, when a suitable match can be identified between the available liquid filter and the solar cell, a spectrally selective liquid absorption filter provides a reduced cost potential as a spectrum beam splitter in the PV/T systems [13].

A wide variety of studies were performed in the previous years that concerned about the selection criteria of the absorptive-based filters and their influence on either the PV or PV/T modules performance. For instance, Chendo et al. [15] were the first who investigated the liquid optical filter for use in solar energy conversion. Their findings indicated that cobalt sulphate salt may be a preferable option for PV/T modules that utilized silicon solar cells. Also, Barnett and Wang [16] constructed and optimized a spectrum beam splitting PV system for GaInP/GaAs, Si, and GaInAsP/GaInAs cells using dichroic filtering, attaining a 39.1 % efficiency at a concentration ratio of 30. Additionally, Sabry et al. [17] reported that an ideal fluid filter may significantly improve the efficiency of a solar cell by approximately

30% and 40% of the solar radiation that can be captured as a thermal energy by the filter. Likewise, the durability of different heat transfer fluids was investigated by Looser et al. [18] over UV radiation exposure at 75 and 150°C. Among the proposed fluids, the industrial-grade propylene glycol with a chemically inert red dye was shown to be the optimum filter. Latterly, a filter that combines a dichroic solid filter ($\text{SiO}_2/\text{TiO}_2$) and a heat transfer fluid was further developed by Mojiri et al. [19]. For silicon cells, their preferred spectral range was 600-1125 nm. The thermal absorber received the remaining 54.5 % of the focused light, which was then converted by the filter to electricity with a percentage of 26.1 % and sent to the cells. Based on the brief previous literatures, it can be found that several investigations have examined and compared numerous optical filters whether being associated with the PV or PV/T structures aiming to demonstrate their effectiveness and influence on the overall performance along with indicating the generated thermal or electric powers.

Consequently, the Monte Carlo method is adopted for the purpose of evaluating and comparing the performance of two different optical filters implemented with a PV module. Both configurations are designed such that the PV module is coupled with a static working fluid enclosed between two layers of an optical glass named as K9, which is the optical filter. Moreover, one of the proposed structures utilizes water as a working fluid between the glass layers, while the other uses glycerin.

Else, the generated electrical power and efficiency are compared for both of the suggested configurations and the stand-alone PV unit.

2. SYSTEM DESIGN AND EXPERIMENTAL PROCEDURES

In this section, the specifications of the suggested modules, the experimental setup description and the governing equations used in the current analysis are discussed in details.

2.1. System description

The proposed structures are created by locating the optical filter just above the PV panel. The optical filter consists of two layers of an optical glass named as K9, with the space between them filled with a static fluid, which is suggested to be water or glycerin in the current research. Thus, a PV unit with dimensions of 32 x 23 cm² is adopted in the present work, where the optical filter has similar dimensions to those for the PV panel positioned below it. In addition, each layer of the optical glass has a thickness of 6 mm, besides that the space between both glass layers that is filled with a static fluid possess a 4 mm thickness. It should be mentioned that the compositions of the K9 optical glass are SiO_2 , B_2O_3 , Na_2O , K_2O , BaO and As_2O_3 , respectively, with percentages of 69.13, 10.75, 10.4, 6.29, 3.07 and 0.36 %. The stand-alone PV module is labeled as (PV-I), while the structure with an optical filter using water is named as (PV-II) and that employing glycerin is denoted by (PV-III).

As shown in [Fig. 1](#), the experimental setup consists of 6 lambs for the purpose of achieving a constant radiation source using tungsten halogen lamp. The height of

the radiation source is 60 mm from the optical filter and the optical filter is located above the PV panel which has a thickness 16 mm. The lowest part is the PV panel which has a thickness of 30 mm.

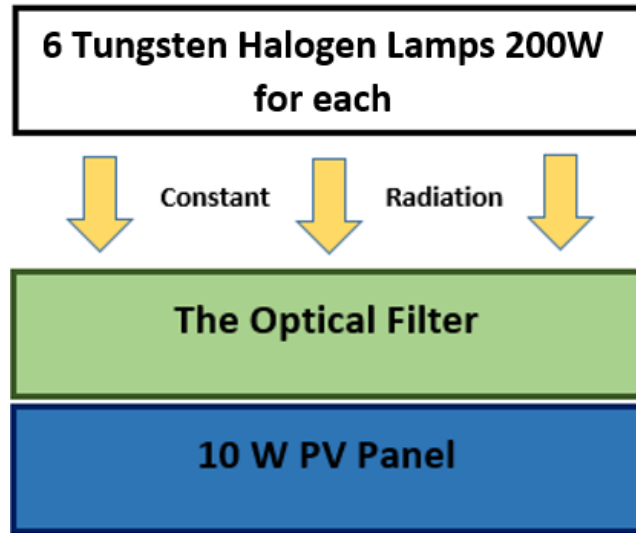


Figure 1. Schematic diagram for the proposed configuration.

[Table 1](#) shows the measuring instruments used in the present experimental work.:

Table 1 List of the measuring instruments.

Measuring Instruments
Digital Multimeter UT136+Series
Digital Temperature Sensor DS18B20
Pyranometer RIKA RK-200-03 sensor with output signal mV
Arduino Mega 2560

2.2. Governing equations

According to the Mie scattering theory, optical filters could be able to absorb a portion of the spectrum, they can also be efficient selective absorbers by utilizing the appropriate base fluid [14]. Excellent heat absorption in spectrum regions that the PV cells are unable to capture is provided by the fluid synergy. The following equations can be used to compute the spectrum fraction transmitted to both the PV cells and optical filters [19-21]:

$$G_{th}(\lambda) = G_{in}(\lambda)\alpha_{OF}(\lambda) \quad (1)$$

$$G_{PV}(\lambda) = G_{in}(\lambda)\tau_{OF}(\lambda) \quad (2)$$

$$Gr_{PV}(\lambda) = G_{in}(\lambda)\gamma_{OF}(\lambda) \quad (3)$$

Where $\alpha_{OF}(\lambda)$ and $\tau_{OF}(\lambda)$ refer to the absorptivity and transmittivity of the optical filter, respectively, whereas $G_{in}(\lambda)$ is the incident spectral energy distribution. Moreover, the spectral fraction absorbed by the thermal absorber is indicated by $G_{th}(\lambda)$ and $Gr_{PV}(\lambda)$ is the spectral fraction reflected to the PV cells, while the reflectivity of the optical filter is given by the symbol $\gamma_{OF}(\lambda)$. It should be clarified that the absorbed solar energy by the optical fluid can be indicated by integrating $G_{th}(\lambda)$ over the wavelength range of 280–4000 nm.

By using the electric power equation and electrical efficiency for as the following [5]:

$$\eta_{ele} = \frac{E_{ele}}{E_s} = \eta_{ref} [1 - \delta_{sc}(T_{sc} - T_{ref})] \quad (4)$$

$$E_{ele} = \eta_{sc} A_{sc} G_{sc} [1 - \delta_{sc}(T_{sc} - T_{ref})] \quad (5)$$

Where E_{ele} is the produced electric power from the PV module, η_{sc} refers to the PV cell efficiency at the reference temperature, A_{sc} is the PV cell surface area, G_{sc} refers to the portion of incoming solar radiation that reaches the PV cell by taking into account the solar cell absorptivity, the above layer transmissivity, and the PV module packing factor. δ_{sc} is the temperature coefficient for the crystalline silicon cell. T_{sc} and T_{ref} refer to the solar cell temperature and the reference temperature, respectively.

2.3. Experimental procedure

An experimental setup is established with the intention of monitoring the PV surface temperature in order to be able to calculate the PV generated electrical power and the efficiency of a stand-alone PV module along with both the explored layouts employing water and glycerin as working fluids. Thus, a 200 W constant radiation heat source is developed and mounted at a height of 60 mm above a 10 W PV panel by utilizing the current-voltage and current-power curves supplied by SOLARTECH company as shown in [Fig. 2](#).



Figure 2. Experimental setup.

2.3. Monte Carlo approach

The Monte Carlo Method is a broad category of computational techniques that involves periodic random sampling to get numerical results. The fundamental concept is to use randomness to solve problems that, in principle, may be deterministic.

They are commonly used to solve mathematical and physical issues, and they are incredibly beneficial when using different approaches that would be difficult or impossible to be solved. Where Monte Carlo methods are most commonly used in three problem classes of numerical integration, creating draws from a probability distribution, and optimization. For the purpose of determining the efficiency of a fluid as a band-pass filter, the following partitioned integral can be drawn [22, 23]:

$$\eta = \frac{\int_{short\lambda}^{long\lambda} E_{\lambda} T_{\lambda} d\lambda}{\int_{short\lambda}^{long\lambda} E_{\lambda} d\lambda} - \frac{\int_0^{short\lambda} E_{\lambda} T_{\lambda} d\lambda}{\int_0^{short\lambda} E_{\lambda} d\lambda} - \frac{\int_{long\lambda}^{4\mu m} E_{\lambda} T_{\lambda} d\lambda}{\int_{long\lambda}^{4\mu m} E_{\lambda} d\lambda} \quad (6)$$

Where E_{λ} describes the amount of solar irradiance per unit wavelength with its value obtained from Gueymard [24]. A perfectly transparent filter ($T=1$) between the short and long wavelengths that differs according to the type of cell will achieve an efficiency of 1. Accordingly, this objective function can be used for filter optimization. Consequently, the present study utilizes a simple Monte Carlo approach to randomly generate volume fraction combinations which can be referred by η to find the optimum filter [22]. Relying to the previously mentioned concept, the efficiency can be estimated by using this equation. However, it should be realized that this equation was developed on the basis of ideal filter which covers the entire spectrum for various types of PV cells.

3. RESULTS AND DISCUSSION

The performance of two distinct optical filters combined with a PV module is evaluated and compared in the present study using the Monte Carlo approach. The PV module is associated with a static working fluid encapsulated between two layers of an optical glass known as K9, which serves as the optical filter in both the proposed setups.

The water is utilized as a working fluid in one module, while the glycerin is used in the other one. Additionally, the electric power and efficiency for both modules with optical filters are analyzed and compared with those for the PV unit with no optical filter experimentally.

The ambient temperature changes significantly from 25°C at the beginning of the experiment to increase by about 2°C after passing 600 seconds.

3.1. The optical properties for the proposed arrangements

The changes in the percentages of absorbance for water and glycerin as optical filters are shown in Fig. 3 across the spectrum wavelength that ranges from 190 to 2500 nm. It is clearly obvious from this figure that the absorbance percentage is increasing at the wavelength region from 190 to 300 nm for both filters, which is a favorable absorbance for UV range as this can cause an elevation in the temperature of PV cell. Whereas, a sharp reduction happens throughout the range from 360 to 1200 nm which is a beneficial range for the purpose of generating the electricity from the crystalline PV cells. On the other hand, the water as a working fluid reveals a significant lower absorbance percentage than that for the glycerin in the IR range.

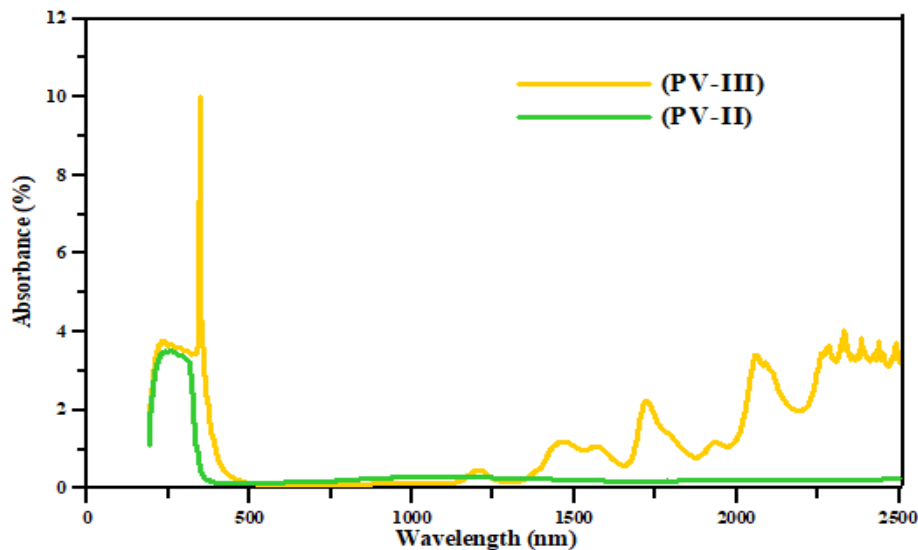


Figure 3. Variations in the absorbance of water and glycerin between 190 and 2500 nm.

Fig. 4 presents the variations in the transmittances for water and glycerin. As depicted from this figure, both working fluids have a slightly similar transmittance

percentage across both the UV and IR ranges, which are very low. It should be emphasized that both of these ranges are unfavorable since they considerably raise the PV cell temperature. However, from 360 to 500 nm it nearly for each other and from 500 to 1000 nm the bottoms and domes get a differences form water and glycerin with the last range from 1000 to 1500 nm the difference is much bigger than before. Also, the data measured by JASCO Spectrophotometer V-570 which has a wavelength accuracy for UV/VIS region ± 0.1 nm (at a spectral bandwidth of 0.5 nm) and for NIR region ± 0.4 nm (at a spectral bandwidth of 0.2 nm)

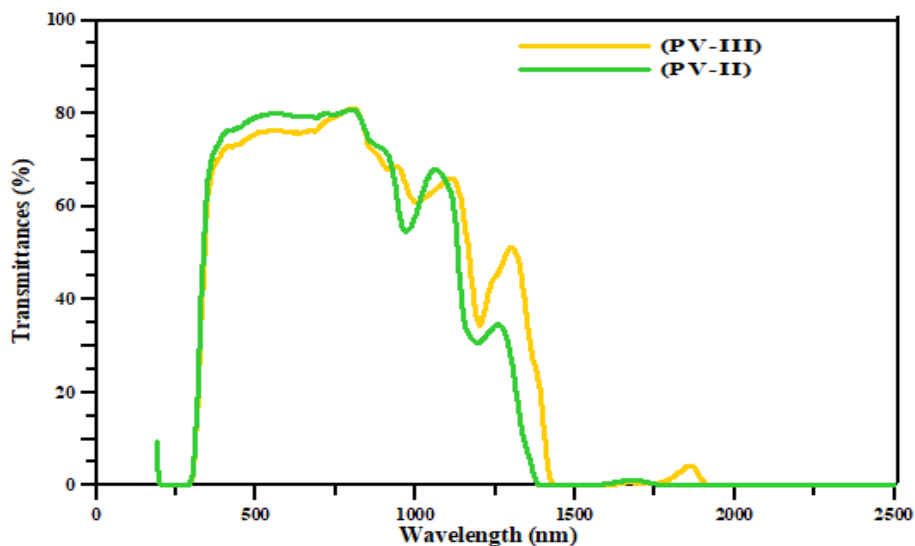


Figure 4. Changes in the transmittances of optical filters between 190 and 2500 nm.

It is clearly obvious from [Fig. 5](#) that the spectral irradiance of both filters is dramatically less than the total spectrum with a slight difference between the investigated filters, as the total spectrum accounts for a perfect transmittance which equals to 1, whereas the transmittances of both filters actually do not reach to 1. It

is apparently shown from this figure that the average area under curve for the (PV-II) module is somewhat greater than (PV-III) with values of 637.4 and 631 W/m² for (PV-II) and (PV-III) layouts, respectively, along the wavelength range from 280 to 2500 nm.

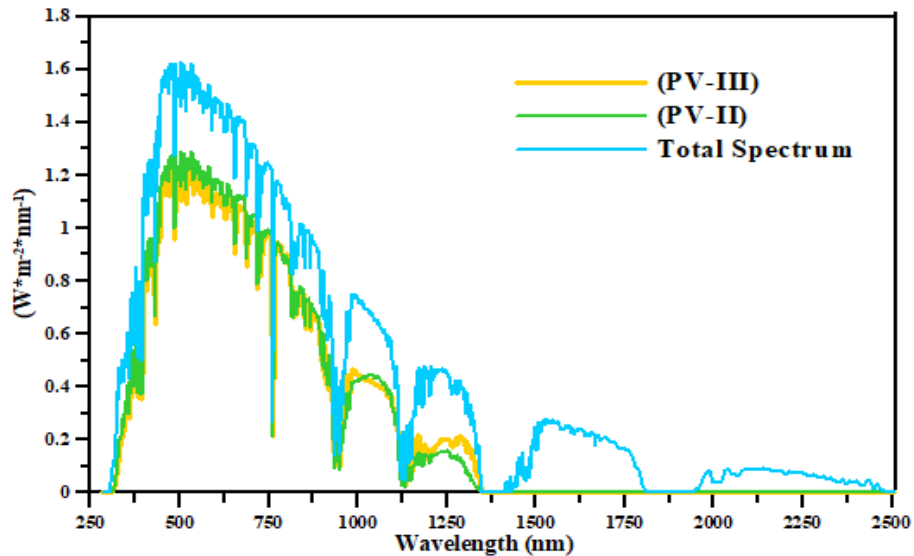


Figure 5. The spectral irradiance of the proposed filters and AM 1.5 total spectrum between 280 and 2500 nm.

Fig. 6 displays the trend of variation of the spectral irradiance for the Monte Carlo ideal filter and total global spectrum Am 1.5. Firstly, the Monte Carlo concept for ideal filter can be found in the working range for the crystalline PV cell. Moreover, the range at which the cell can be capable to convert the falling spectrum for every wavelength in to a useful electrical power is from 360nm to 1100nm. It should be noted that every optical filter should be compared to the ideal filter presented by the Monte Carlo concept. Thus, Monte Carlo ideal filter should first be displayed in order to assess the effectiveness of the optical filters that are

discussed in the current research. Additionally, this approach assumes that the ideal filter has a perfect transmittivity for the solar cell spectrum range which in the present study ranges from 360nm to 1100nm. Consequently, the efficiency of the optical filter adopting water is dramatically higher than that using glycerin with values of 60.02% and 53.8% for water and glycerin, respectively, using the Monte Carlo point of view as depicted in Eq. (4).

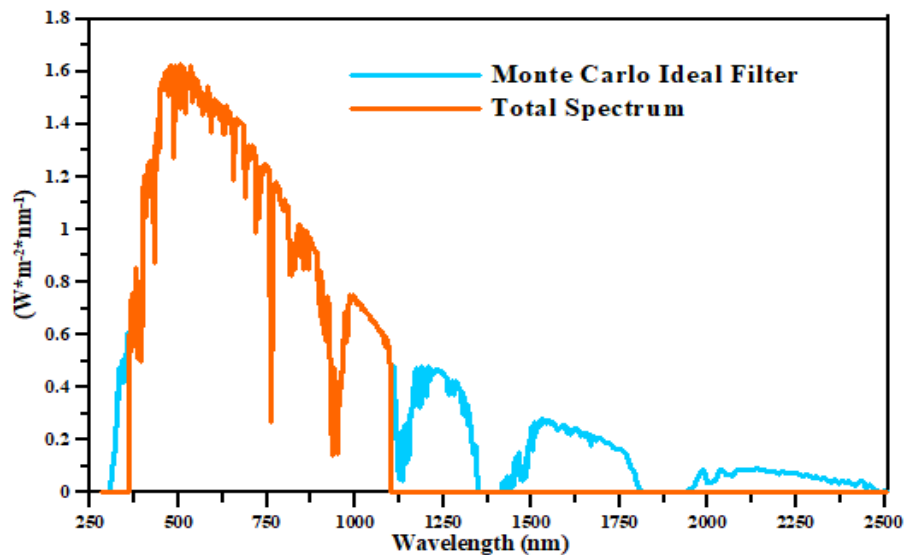


Figure 6. The variations of spectral irradiance for the total spectrum and Monte Carlo ideal filter in the range between 280 to 2500 nm.

3.2. Performance evaluation

The changes of the PV module surface temperature with time for the modules with optical filters and those without are illustrated in Fig. 7. It is clearly obvious from this figure that the temperature significantly boosts with time for all modules. As the optical filter using water greatly absorbs the unfavorable band of spectral irradiance, the lowest PV surface temperature is revealed via this module. After

passing 100 sec, the temperatures for the modules with optical filters are slightly the same with values considerably lower than those offered by the stand-alone PV module. However, the (PV-I) module achieves the highest surface temperature followed by the (PV-III) and (PV-II) configurations, respectively, with values of 150.8, 67.4 and 61.65 °C, after passing 600 sec.

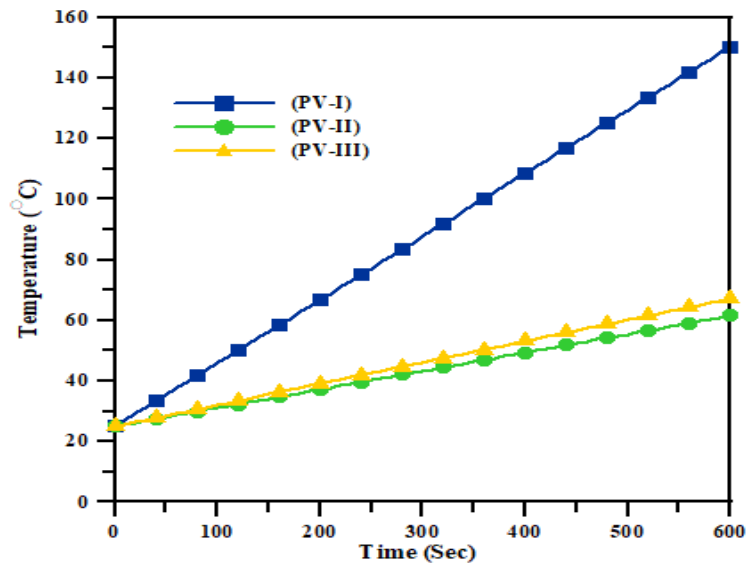


Figure 7. The temperature variations with time for the PV module surface of the investigated layouts.

Fig. 8 illustrates the electrical power variations with time for the presented configurations. It is significantly shown from this figure that the electrical power dramatically enhances with time for all structures. The highest electrical power is provided by the PV module adopting water followed by that employing glycerin and the stand-alone PV module, respectively.

The reason for this is that the temperature declination greatly raises the PV module output electrical power. After 600 sec, the generated electrical powers are

approximately 1.54, 2.47 and 2.53, respectively, for the (PV-I), (PV-III) and (PV-II) arrangements.

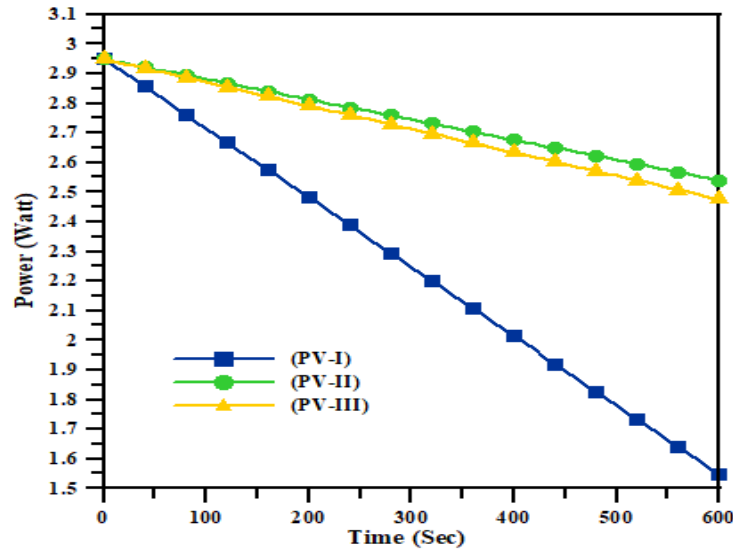


Figure 8. The generated electrical power variations with time for the suggested arrangements.

The electrical efficiencies are obviously reduced with passing time for all modules as seen in Fig. 9. This because of the significant declination of the electrical power as shown in Fig. 8 for the reasons mentioned previously. Thus the (PV-II) structure acquires the highest electrical efficiency that reaches to about 4%, followed by the (PV-III) and (PV-I) layouts, with values of 3.91 and 2.42%, respectively.

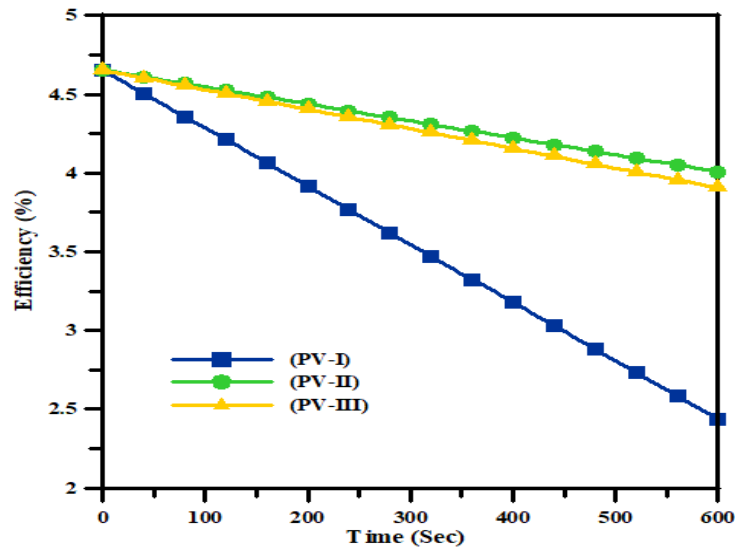


Figure 9. The electrical efficiencies variations with time for the presented setups.

4. CONCLUSIONS

The impact of locating an optical filter above the PV module is studied and compared with the stand-alone PV unit in the current research. Both arrangements are obtained such that a static working fluid that is placed between two layers of K9 optical glass. Likewise, glycerin is used in one of the suggested systems, while the other includes water as the working fluid between the glass layers. Else, the PV module electrical power, surface temperature and efficiency are compared for the proposed configurations and the stand-alone PV module. The following conclusions can be drawn:

- 1- The efficiency of the optical filter adopting water is marginally greater than that using glycerin by applying the Monte Carlo approach.
- 2- The water as a static working fluid provides a lower absorbance percentage than that for the glycerin in the IR range.

- 3- Following the stand-alone PV module with values of 150.8, 67.4 and 61.65 °C, respectively, the configurations incorporating optical filters with glycerin and water obtain the greatest surface temperatures.
- 4- The structure employing water as an optical filter acquires the highest electrical efficiency that is 4%, followed by the layout using glycerin and the PV unit with no optical filter, with values of 3.91 and 2.42%, respectively.

REFERENCES

- [1] B. Looney, Statistical review of world energy, 2020, Bp 69 (2020) 66.
- [2] T. Ma, H. Yang, L. Lu, J. Peng, Technical feasibility study on a standalone hybrid solar-wind system with pumped hydro storage for a remote island in Hong Kong, *Renewable energy* 69 (2014) 7-15.
- [3] U. Stritih, Increasing the efficiency of PV panel with the use of PCM, *Renewable Energy* 97 (2016) 671-679.
- [4] H. Fayaz, N. Rahim, M. Hasanuzzaman, R. Nasrin, A. Rivai, Numerical and experimental investigation of the effect of operating conditions on performance of PVT and PVT-PCM, *Renewable Energy* 143 (2019) 827-841.
- [5] M. Abd El-Hamid, G. Wei, M. Sherin, L. Cui, X. Du, Comparative Study of Different Photovoltaic/Thermal Hybrid Configurations From Energetic and Exergetic Points of View: A Numerical Analysis, *Journal of Solar Energy Engineering* 143 (2021) 061006.
- [6] J.-L. Lim, S.-C. Woo, T.-H. Jung, Y.-K. Min, C.-S. Won, H.-K. Ahn, Analysis of factor on the temperature effect on the output of PV module, *The Transactions of The Korean Institute of Electrical Engineers* 62 (2013) 365-370.
- [7] M. Abd El-Hamid, G. Wei, L. Cui, C. Xu, X. Du, Three-dimensional heat transfer studies of Glazed and Unglazed Photovoltaic/Thermal systems embedded with Phase Change Materials, *Applied Thermal Engineering* (2022) 118222.
- [8] T. Ma, H. Yang, Y. Zhang, L. Lu, X. Wang, Using phase change materials in photovoltaic systems for thermal regulation and electrical efficiency improvement: a review and outlook, *Renewable and Sustainable Energy Reviews* 43 (2015) 1273-1284.
- [9] E. Radziemska, The effect of temperature on the power drop in crystalline silicon solar cells, *Renewable energy* 28 (2003) 1-12.
- [10] S. Tang, H. Hong, H. Jin, Y. Xuan, A cascading solar hybrid system for co-producing electricity and solar syngas with nanofluid spectrum selector, *Applied Energy* 248 (2019) 231-240.
- [11] K. Wang, M. Herrando, A.M. Pantaleo, C.N. Markides, Technoeconomic assessments of hybrid photovoltaic-thermal vs. conventional solar-energy systems: Case studies in heat and power provision to sports centres, *Applied Energy* 254 (2019) 113657.

- [12] X. Han, D. Xue, J. Zheng, S.M. Alelyani, X. Chen, Spectral characterization of spectrally selective liquid absorption filters and exploring their effects on concentrator solar cells, *Renewable energy* 131 (2019) 938-945.
- [13] P.R. Jiwanapurkar, S.S. Joshi, A review on fluid based beam splitters for solar photovoltaic/thermal system, *Int J Recent Innov Trends Comput Commun* 3 (2015).
- [14] G. Huang, S.R. Curt, K. Wang, C.N. Markides, Challenges and opportunities for nanomaterials in spectral splitting for high-performance hybrid solar photovoltaic-thermal applications: a review, *Nano Materials Science* 2 (2020) 183-203.
- [15] M. Chendo, D. Osborn, R. Swenson. Analysis of spectrally selective liquid absorption filters for hybrid solar energy conversion. in *Optical Materials Technology for Energy Efficiency and Solar Energy Conversion IV*. 1985. SPIE.
- [16] A. Barnett, X. Wang. High efficiency, spectrum splitting solar cell assemblies: Design, measurement and analysis. in *Optics for Solar Energy*. 2010. Optica Publishing Group.
- [17] M. Sabry, R. Gottschalg, T.R. Betts, M. Shaltout, A. Hassan, M. El-Nicklawy, D. Infield. Optical filtering of solar radiation to increase performance of concentrator systems. in *Conference Record of the Twenty-Ninth IEEE Photovoltaic Specialists Conference, 2002*. 2002. IEEE.
- [18] R. Looser, M. Vivar, V. Everett, Spectral characterisation and long-term performance analysis of various commercial Heat Transfer Fluids (HTF) as Direct-Absorption Filters for CPV-T beam-splitting applications, *Applied energy* 113 (2014) 1496-1511.
- [19] A. Mojiri, C. Stanley, R.A. Taylor, K. Kalantar-Zadeh, G. Rosengarten, A spectrally splitting photovoltaic-thermal hybrid receiver utilising direct absorption and wave interference light filtering, *Solar Energy Materials and Solar Cells* 139 (2015) 71-80.
- [20] K. Wang, I. Pasmazoglou, B. Franchetti, M. Herrando, A. Pantaleo, C. Markides. Thermoeconomic assessment of a spectral-splitting hybrid PVT system in dairy farms for combined heat and power. in *Proc. Int. Conf. Effic., Cost, Optim., Simul. Environ. Impact Energy Syst*. 2019.
- [21] C. Shou, Z. Luo, T. Wang, W. Shen, G. Rosengarten, W. Wei, C. Wang, M. Ni, K. Cen, Investigation of a broadband TiO₂/SiO₂ optical thin-film filter for hybrid solar power systems, *Applied Energy* 92 (2012) 298-306.
- [22] R.A. Taylor, T. Otanicar, G. Rosengarten, Nanofluid-based optical filter optimization for PV/T systems, *Light: Science & Applications* 1 (2012) e34-e34.
- [23] X. Han, X. Chen, Y. Sun, J. Qu, Performance improvement of a PV/T system utilizing Ag/CoSO₄-propylene glycol nanofluid optical filter, *Energy* 192 (2020) 116611.
- [24] C.A. Gueymard, Parameterized transmittance model for direct beam and circumsolar spectral irradiance, *Solar Energy* 71 (2001) 325-346.